DOE/ET/53088/1-R IFSR #1-R

ANOMALOUS ION CONDUCTION FROM TOROIDAL DRIFT MODES

Wendell Horton

Institute for Fusion Studies
The University of Texas at Austin
Austin, Texas 78712

Revised November 1981

ANOMALOUS ION CONDUCTION FROM TOROIDAL DRIFT MODES

Wendell Horton

Institute for Fusion Studies &
Department of Physics
The University of Texas at Austin
Austin, Texas 78712

Abstract

The anomalous ion thermal transport produced by the toroidal drift wave instability is analyzed for finite amplitude single modes and the transition to turbulent flows.

Revised November 1981

To be published in
Plasma Physics (January 1982)

I. INTRODUCTION

Based on computer simulations[1] and analytic studies[2], a simple nonlinear description of the ion pressure gradient instability in toroidal geometry has been introduced. The instability is described locally on the outside of the torus by two coupled nonlinear partial differential equations for the electrostatic potential and pressure fluctuation.

In the study of Horton, et al.[2] the renormalized turbulence theory is used to obtain a model wavenumber spectrum, the saturation level, and, in the saturated state, a final result for the turbulent thermal conductivity. The turbulence theory is based on a statistical description of the weakly interacting fluctuations. In fact, closure of the equation for the spectral distribution is obtained by neglecting intrinsic four-field correlation effects.

In this work we consider a simpler calculation based on the opposite assumption. Namely, we consider that the system is sufficiently close to marginal stability that only one mode, along with its coherent harmonic components, needs to be considered. This condition of weak instability can be guaranteed by considering a discrete azimuthal wavenumber spectrum $k_y = 2\pi m/L_y = m/r$ due to periodicity in y and pushing the system parameters just past marginal stability. For such a temperature gradient only the mode k satisfies the dispersion relation and is linearly unstable.

The situation is shown in Fig. 1. The first bifurcation point is an exchange of stability where the two stable oscillations $\omega_{\pm}(k,\eta)$ for $\eta < \eta_c$. As we proceed to larger values of the temperature gradient η, a sequence of modes are destabilized. The second bifurcation is at η_1 with the subsequent sequence $\eta_2, \eta_3, \ldots$ leading to complicated solutions which eventually become stochastic in nature.

The Hopf bifurcation theory[4] implies that in the neighborhood of each of these critical points there emerges a new stable limit cycle. Here we calculate the limit cycle, the nonlinear phase shift and the thermal conduction in the neighborhood of the first bifurcation. Procedures are given by Keller[4], for example, for systematically constructing the bifurcation diagram shown here schematically in Fig. 1. The method is constructive and involves solving the nonlinear eigenvalue problem defined by the finite amplitude steady state equations.

In Section III we analyze the convective heat flux carried by the coherent oscillatory flows. Recent neutral fluid experiments on the transition to turbulence appear to show that typically only a few bifurcations are observed before the onset of stochastic fluctuations. In Sections IV and V we consider the conditions required for the onset of stochasticity in the flow that circulates between convective cells swirling in opposite directions. Finally,

we discuss observations in neutral fluid experiments which support the picture of the onset of turbulent flow developed in this article.

II. LIMIT CYCLE AT THE FIRST BIFURCATION POINT

We consider that a parameter, particularly the ion temperature gradient, has increased to push the system into the unstable regime. We now calcuate perturbatively through the third order in the amplitude of the oscillations the nonlinear fields in the system. At third order we obtain a secular component which determines the nonlinear amplitude of the oscillations. From Hopf bifurcation theory we expect to find the frequency to be given by that of the linear oscillations at marginal stability and the amplitude to be directly proportional to $(\eta - \eta_c)^{\frac{1}{2}}$ measuring the excess of the temperature gradient that drives the instability.

The nonlinear equations[2] for the fluctuations in the system are

$$\frac{\partial \varphi}{\partial t} = -\hat{u} \frac{\partial \varphi}{\partial y} + 2\varepsilon_n \frac{\partial}{\partial y} \delta p \qquad (1)$$

$$\frac{\partial \delta p}{\partial t} = -(1 + \eta) \frac{\partial \varphi}{\partial y} - [\varphi, \delta p] \qquad (2)$$

which reflect the statements of $\nabla \cdot \underset{\sim}{j}_{\perp} = 0$ and $dp_i/dt = 0$, respectively. The parameters of the system are the temperature-to-density gradient ratio $\eta = d\ell nT/d\ell nn$, the inverse aspect ratio $\varepsilon_n = r_n/R$ and the electron drift wave azimuthal phase velocity $u_k = 1 - (1 + \eta)k^2$. The dependence of the instability on the magnetic shear and the connection length is given in Horton, Choi and Tang[2] and is neglected here. Kinetic theory effects, particularly

the change in the phase velocity u_k of the drift wave due to the velocity space average of the finite Larmor radius factor $J_0^2(k_\perp v_\perp/\omega_{ci})$, are investigated for this instability by Coppi and Pegoraro[5].

For the truncated $\underset{\sim}{k}$ spectrum the nonlinear equations (1) and (2) may be written as

$$\frac{d\varphi(\underset{\sim}{k})}{dt} = -iku_k\varphi(\underset{\sim}{k}) + i2\varepsilon_n k\delta p(\underset{\sim}{k}) \tag{3}$$

$$\frac{d\delta p(\underset{\sim}{k})}{dt} = -ik(1+\eta)\varphi(\underset{\sim}{k}) + \sum_{\underset{\sim}{k}_1+\underset{\sim}{k}_2=\underset{\sim}{k}} \hat{z}\cdot\underset{\sim}{k}_1 \times \underset{\sim}{k}_2\varphi(\underset{\sim}{k}_1)\,\delta p(\underset{\sim}{k}_2) \,. \tag{4}$$

In the absence of the nonlinear mode coupling it is straightforward to show that the collective fluctuations are given by

$$\varepsilon_{\underset{\sim}{k}}(\omega) = \omega(\omega - ku_k) + k^2\gamma_0^2 = 0 \tag{5}$$

and are unstable when $2\gamma_0 > |u_k|$. Here, we define $\gamma_0 = [2\varepsilon_n(1+\eta)]^{\frac{1}{2}}$ as in Horton, Choi and Tang[2]. The most unstable wavenumber is given by

$$k_0 = (1+\eta)^{-\frac{1}{2}} \,, \tag{6}$$

and the unstable wavenumber band is given by

$$k_0(1-2\gamma_0)^{\frac{1}{2}} < k < k_0(1+2\gamma_0)^{\frac{1}{2}} \,. \tag{7}$$

For $\gamma_0 > 1/2$ the unstable band extends from $k=0$ to $k_0(1+2\gamma_0)^{\frac{1}{2}}$.

For a discrete azimuthal wavenumber spectrum, $k=m/r$, in a periodic system the mode number m with k closest to k_0 is the first mode to become unstable. Let us write

the small amplitude oscillations at the wavenumber nearest k_0 as

$$\varphi^{(1)} = a\Phi(x)\cos[k(y - ut)] \tag{8}$$

and

$$\delta p^{(1)} = a\chi_0\Phi(x)\cos[k(y - ut) - \phi] \tag{9}$$

where we consider that

$$\Phi(x) = \sin(qx)$$

with q given by the geometry. In the linear approximation the two complex equations (1) and (2) determine the unknowns a, ϕ, u, χ_0. Substituting (8) and (9) into (1) and (2) yields the four equations

$$ku = ku_k - 2\varepsilon_n k\chi_0 \cos\phi \tag{10}$$

$$\frac{da}{dt} = 2\varepsilon_n ka\chi_0 \sin\phi \tag{11}$$

$$\frac{da}{dt}\cos\phi = kau \sin\phi \tag{12}$$

$$\chi_0 \frac{da}{dt}\sin\phi + a\chi_0 ku \cos\phi = (1 + \eta)ka \tag{13}$$

to the first order in $a(t)$. In the Appendix we describe a more general form of the solution which allows for a time dependence in the relative phase ϕ.

We now assume that the nonlinear fields can be calculated by a small amplitude expansion

$$\varphi = \varphi^{(1)} + \varphi^{(2)} + \varphi^{(3)} + \ldots \tag{14}$$

$$\delta p = \delta p^{(1)} + \delta p^{(2)} + \delta p^{(3)} + \ldots \tag{15}$$

where

$$|\varphi^{(n)}| \sim |\delta p^{(n)}| \sim a^n \tag{16}$$

with $a << 1$. We substitute the expansion (14), (15) into equations (1) and (2) and solve order by order.

The first order equations are equivalent to the stability analysis of the equilibrium. The equilibrium $a = da/dt = 0$ is stable or unstable according to $2\gamma_0 \lesseqgtr |u_k|$, respectively. In summary, we have from equations (10) through (13) the two cases:

(i) $2\gamma_0 < |u_k|$

$$\chi_0 = (1 + \eta)/u$$

$$\sin\phi = 0$$

$$u^2 - uu_k + \gamma_0^2 = 0 \tag{17}$$

or

$$u = \frac{1}{2}u_k \pm \left(\frac{1}{4}u_k^2 - \gamma_0^2\right)^{\frac{1}{2}}$$

(ii) $2\gamma_0 > |u_k|$

$$\cos\phi = u_k/2\gamma_0$$

$$\sin\phi = \left(1 - u_k^2/4\gamma_0^2\right)^{\frac{1}{2}}$$

$$u = \frac{1}{2}u_k \quad \text{and} \quad \gamma_k = k\gamma_0 \sin\phi$$

$$\chi_0 = [(1 + \eta)/2\varepsilon_n]^{\frac{1}{2}} \tag{18}$$

A. Second-Order Fields

We now calculate the effect of the nonlinear convection associated with the first-order fields by evaluating

$$\underset{\sim}{v}_E \cdot \nabla \delta p = [\varphi, \delta p] \equiv \frac{\partial \varphi}{\partial x}\frac{\partial \delta p}{\partial y} - \frac{\partial \varphi}{\partial y}\frac{\partial \delta p}{\partial x} .$$

Using equations (8) and (9) and defining the phase variable $\Theta = k(y - \hat{u}t)$, we obtain

$$[\varphi^{(1)}, \delta p^{(1)}] = \frac{1}{2} a^2 \chi_0 kq \sin(2qx) \times [\sin\Theta \cos(\Theta - \phi) - \cos\Theta \sin(\Theta - \phi)]$$

$$= \frac{1}{2} a^2 \chi_0 kq \sin(2qx) \sin\phi . \qquad (19)$$

As is well known, the convective nonlinearity only produces the difference of the azimuthal wavenumbers, which is at $k"=0$ for the self-interaction. The second-order fields are given by

$$\frac{\partial}{\partial t}\varphi^{(2)} = -\hat{u}\frac{\partial \varphi^{(2)}}{\partial y} + 2\varepsilon_n \frac{\partial}{\partial y}\delta p^{(2)} \qquad (20)$$

$$\frac{\partial}{\partial t}\delta p^{(2)} = (1 + \eta)\frac{\partial \varphi^{(2)}}{\partial y} - \frac{1}{2} a^2 \chi_0 kq \sin(2qx) \sin\phi . \qquad (21)$$

The solutions are evidently

$$\varphi^{(2)} = 0$$

$$\delta p^{(2)}(x,t) = -\frac{1}{2} \chi_0 kq \sin\phi \sin(2qx) \int^t a^2 dt' . \qquad (22)$$

The second-order fields are uniform in y and give a steepened x gradient to the pressure fluctuation.

B. Third-Order Fields

The convective derivative acting on the second-order fields reduces to

$$[\varphi,\delta p]^{(3)} = [\varphi^{(2)},\delta p^{(1)}] + [\varphi^{(1)},\delta p^{(2)}]$$

$$= [\varphi^{(1)},\delta p^{(2)}] = -\frac{\partial \varphi^{(1)}}{\partial y}\frac{\partial \delta p^{(2)}}{\partial x} .$$

Since $\varphi^{(2)} = 0$ there is simply a reaction in the pressure equation due to the first-order flow v_{Ex} convection of the second-order pressure fluctuation.

The third-order equations are

$$\frac{\partial}{\partial t}\varphi^{(3)} = -\hat{u}\frac{\partial \varphi^{(3)}}{\partial y} + 2\varepsilon_n \frac{\partial}{\partial y}\delta p^{(3)} \tag{23}$$

$$\frac{\partial}{\partial t}\delta p^{(3)} = -(1+\eta)\frac{\partial \varphi^{(3)}}{\partial y} + \frac{\partial \varphi^{(1)}}{\partial y}\frac{\partial \delta p^{(2)}}{\partial x} \tag{24}$$

where

$$[\varphi^{(1)},\delta p^{(2)}] = -\frac{1}{2}\chi_0 k^2 q^2 \sin\phi\,[\sin(3qx) - \sin(qx)]$$

$$\sin\Theta\, a(t)\int^t a^2(t')dt" . \tag{25}$$

Returning to the first-order equations and collecting the components that vary as $\cos\Theta$ and $\sin\Theta$, we again obtain equations (1) through (12) and the nonlinear modification to equation (13) given by

$$\chi_0 \frac{da}{dt}\sin\phi + a\chi_0 ku\cos\phi = (1+\eta)ka$$

$$-\frac{1}{2}\chi_0 k^2 q^2 \sin\phi\, a\int^t a^2(t')dt' . \tag{26}$$

Using the relations in case (ii) equation (18), we now reduce equation (26) to obtain

$$\frac{da}{dt} = \left[k\gamma_0 \sin\phi - \frac{k^2 q^2}{2} \int^t a^2(t')dt' \right] a(t) \quad . \quad (27)$$

Equation (27) has an analytic solution found by reducing the equation to

$$\frac{dy}{d\tau} = x \quad (28)$$

$$\frac{dx}{d\tau} = (1 - y)x$$

where $\tau = 2\gamma_k t$ and $x(\tau) = (kq/2\gamma_k)^2 a^2(t)$. The solution is

$$a(t) = \frac{2\gamma_k}{|kq|} \frac{\exp(\gamma_k t)}{1 + \frac{1}{2}\exp(2\gamma_k t)} \quad , \quad (29)$$

and in the limit $t \to +\infty$ the solution has $y = 2$ or

$$\frac{k^2 q^2}{2} \int_{-\infty}^{+\infty} a^2(t')dt' = 2k\gamma_0 \sin\phi = 2\gamma_k \quad . \quad (30)$$

Finally, we note that a more general solution for $a(t)$ is given in the Appendix.

C. Quasilinear Approximation

In the spirit of weak turbulence theory we consider the following approximation for the time history integral,

$$\int^t a^2(t')dt' = \frac{a^2(t)}{2\gamma_k^{\ell}} \quad .$$

In this model the amplitude equation (27) becomes local in time

$$\frac{da}{dt} = \left[k\gamma_0 \sin\phi - \frac{k^2 q^2}{4\gamma_k^{\ell}} a^2(t) \right] a(t) \quad . \qquad (31)$$

Now $a(t)$ approaches a stable limit cycle with

$$a_L^2 = \frac{4(\gamma^{\ell})^2}{k^2 q^2} = \frac{4(\gamma_0^2 - \frac{1}{4} u_k^2)}{q^2}$$

or

$$a_L = \frac{2\left(\gamma_0^2 - \frac{1}{4} u_k^2\right)^{\frac{1}{2}}}{\langle k_x^2 \rangle^{\frac{1}{2}}} = \frac{2\gamma_0 \sin\phi}{q} \quad . \qquad (32)$$

This approximate solution for $a(t)$ is closely related to the turbulence theory formula for the mean square amplitude.

Comparing equations (29) and (32), we find that instead of maintaining $a(t) = a_L$ the integral (nonlocal) equation for $a(t)$ has the long-time behavior

$$\lim_{t\to\infty} a(t) \approx 2a_L \exp(-\gamma_k t) \quad . \qquad (33)$$

Figure 2 describes the parametric dependence of the limiting amplitude on the temperature gradient.

The amplitude formula is extrapolated to large η through the bifurcations shown in Fig. 1 and compared to the result given in Horton, Choi and Tang[2] on the basis of turbulence theory. The root-mean-square level from turbulence theory is smaller by $1/2\sqrt{2}$ than the extrapolated single mode amplitude.

III. THERMAL CONDUCTION

Now we calculate the time-averaged thermal flux Q produced by the nonlinear oscillations. The time average of the locally oscillating flux is also equilvalent to the net flux integrated over the magnetic surface (defined by x = constant) since the oscillations are only a function of $\Theta = k(y - ut)$. The net convective thermal flux is

$$Q(x) = \left\langle v_{Ex} \delta p \right\rangle = -\left\langle \frac{\partial \phi}{\partial y} \delta p \right\rangle \qquad (34)$$

$$= \frac{1}{2} a^2 k \chi_0 \sin^2(qx) \sin\phi$$

as follows from equations (8) and (9).

Here we remark that to model the toroidal system the reference surface $x=0$ is any of the densely packed rational surfaces on which $k_{\|} = (m - \ell q)/qR = 0$. The result of interest for the toroidal system is the summation of Q given in equation (34) over a large number of rational surfaces. Assuming statistical independence on these surfaces the summation becomes

$$a^2 \sin^2(qx) \rightarrow \frac{1}{2} \sum_{m,\ell} |\varphi(m,\ell)|^2 \quad ,$$

where $\varphi(m,\ell)$ is the amplitude $a(t)$ for the mode at the $q(r) = m/\ell$ rational surface. Recent fluid simulations by Brock and Horton[9] show that once the wave amplitudes grow to the level where the resonance overlap criterion derived in Section V is satisfied, the stochastic motion of the

ions across the $\sin(qx)=0$ surfaces eliminates the radial modulation of the radial thermal flux. In the strongly stochastic regime quasilinear theory, with the flux proportional to $\Sigma|\phi(m,\ell)|^2$, is observed in the fluid simulations. An objective of this work is to study the onset of stochasticity in the ion $\underset{\sim}{E}\times\underset{\sim}{B}$ motion of the drift modes.

First we consider the parametric dependence of the flux Q using the limit cycle amplitude a_L obtained in the quasilinear approximation in Section II.B . From equations (18) and (32) we obtain for equation (34)

$$Q = \frac{1}{4}\chi_0 k \frac{4\left(\gamma_0^2 - \frac{1}{4}u_k^2\right)}{q^2}\sin\phi$$

$$= \frac{\gamma_0^2 k}{q^2}\left(\frac{1+\eta}{2\varepsilon_n}\right)^{\frac{1}{2}}\sin^3\phi \quad , \tag{35}$$

with $\sin\phi = (1 - u_k^2/4\gamma_0^2)^{\frac{1}{2}}$. For comparison with the earlier formula[2,3] it is appropriate to approximate k by $k_0 = (1+\eta)^{-\frac{1}{2}}$, the fastest growing mode in a <u>continuous</u> k spectrum, and to define the effective nonlinear thermal conductivity K by

$$Q = K(1+\eta) \quad .$$

The formula for the thermal conductivity that follows from equation (35) is

$$K = \frac{\gamma_0 k}{q^2}\sin^3\phi = \frac{(2\varepsilon_n)^{\frac{1}{2}}}{\langle k_x^2\rangle}\sin^3\phi \quad . \tag{36}$$

with the last reduction obtained using $k = k_0$ from equation (6). Finally, we observe that taking $\sin\phi \simeq 1$ and using $\langle k_x^2 \rangle = (2\varepsilon_n)^{\frac{1}{2}}\xi/q(1+\eta)^{\frac{1}{2}}$ as derived in Horton, Choi and Tang[2] from ballooning mode theory, the formula is

$$K = \frac{q(1+\eta)^{\frac{1}{2}}}{\xi}\left[\frac{\rho}{r_n}\frac{cT}{eB}\right] \tag{37}$$

in the units shown in the brackets. This formula is the same to within a logarithmic factor as that derived earlier from statistical turbulence.[2,3] Here we see that the result follows as the limiting value of the thermal flux when $a(t) \to a_L$ and $\sin\phi \to 1$ from the convection in a single finite amplitude nonlinear oscillation. Of course, in the limit where $2\gamma_0 >> |u_k|$ and $\sin\phi \simeq 1$, the system passes into the region of higher order bifurcations shown in Fig. 1. In Fig. 3 we indicate the dependence of the thermal flux on the stability parameter η.

If the quasilinear model for $a(t)$ is abandoned, then we see from equations (29) and (34) that the flux Q first grows to the value computed from $a = a_L$ and then subsequently decays exponentially. In the regimes of the higher order bifurcations this slow decay is easily interrupted by the presence of mode-mode interactions when their rate for coupling energy is comparable to γ_k^{ℓ}. We conclude that in either case, the value $Q = Q_L$ obtained with $a(t) = a_L$ is an important characteristic value for the thermal conductivity.

The present collisionless theory shows vanishing flux Q at the point of marginal stability $\eta = \eta_c$. To understand the transition from the finite, but small, collisional flux Q_c for $\eta < \eta_c$ to the convective flux for $\eta \gtrsim \eta_c$ we must take into account the small phase shift ϕ between the potential and pressure oscillations in the presence of a finite collisional thermal conductivity. Returning to the linear analysis it is easy to show that the pressure fluctuation equation leads to the phase shift

$$\sin\phi = \frac{k^2\kappa}{ku} = \frac{k\kappa}{\frac{1}{2}u_k} ,$$

when a weak thermal conductivity κ is included in equation (2). For weakly unstable regimes where

$$\sin\phi = \frac{2k\kappa}{u_k} \gg \left(\frac{4\gamma_0^2 - u_k^2}{4\gamma_0^2}\right)^{1/2} \qquad (38)$$

the anomalous flux becomes from equation (35)

$$Q = \frac{2k^2\kappa(\gamma_0^2 - \frac{1}{4}u_k^2)}{u_k q^2} . \qquad (39)$$

The ratio of the convective flux (39) to the conduction

$$Q_c = \kappa(1 + \eta)\ (\rho/r)(cT/eB)$$

is

$$\frac{Q}{Q_c} = \frac{K}{\kappa} = \frac{2k^2(\gamma_0^2 - \frac{1}{4}u_k^2)}{q^2 u_k(1 + \eta)} \qquad (40)$$

which shows the transition from vanishing K/κ at onset to large K/κ in the regime $|u_k| \ll \gamma_0$.

IV. CONVECTION OF PARTICLES IN THE DRIFT MODE

We now calculate the characteristic motion of the guiding centers of the particles in the drift mode given in Section II. For a general potential field $\varphi(x,y,t)$ measured in units of the electron temperature the equations of motion for the guiding center coordinates are Hamilton's equations

$$\frac{dx}{dt} = -\frac{cT_e}{eB}\frac{\partial\varphi}{\partial y}(x,y,t) \tag{41}$$

$$\frac{dy}{dt} = \frac{cT_e}{eB}\frac{\partial\varphi}{\partial x}(x,y,t) \tag{42}$$

with $\varphi(x,y,t)$ for the time-dependent Hamiltonian.

Before the bifurcation point η_1 the drift wave field is characterized by equations (8), (9), and (18). Except for the slow variation of the amplitude $a(t)$, the mode is stationary in the reference frame $y' = y + ut$ where $u = \frac{1}{2}u_k$. In this reference frame, traveling with the phase velocity of the drift mode, the first integral of the equations of motion is

$$\varphi(x,y) = a\sin(qx)\cos(ky) = \varphi_0 = \text{constant} . \tag{43}$$

The contours of constant $\varphi(x,y)$ are shown in Fig. 4. The flows along the contours are given by $\dot{y} = \partial_x\varphi$ and $\dot{x} = -\partial_y\varphi$ in strict analogy to $\dot{q} = \partial_p H$ and $\dot{q} = -\partial_p H$ for one-dimensional nonlinear oscillators. We now calculate the characteristic period τ of the oscillator as a function

of the effective energy φ_0, or here the constant of integration that defines each flow line.

The maxima and minima of $\varphi(x,y)$ occur at $qx_n = (2n + 1)(\pi/2)$ and $ky_m = m\pi$ where $\varphi = \pm a$. Around the maxima and minima there is convection in the clockwise and counter-clockwise directions at the angular frequency

$$\omega_0 = \frac{2\pi}{\tau_0} = \frac{cT_e}{eB} kqa \quad , \tag{44}$$

since the Hamiltonian is harmonic for $|\varphi_0| << a$. The trajectories given by equations (41), (42) and (43) are obtained in terms of the elliptic function $dn(u|m)$ with $u = \omega_0 t$ and $m = 1 - \varphi_0^2/a^2$. We find that

$$\sin[qx(t)] = dn(\omega_0 t|m)$$

$$\cos[ky(t)] = dn(\omega_0 t + K|m)$$

with the full period of circulation given by $\omega_0 \Delta t = 4K$ or

$$\omega(\varphi_0) = \omega_0 \left[\frac{\pi}{2K(m)}\right]$$

$$\cong \begin{cases} \omega_0\left[1 - \frac{1}{4}\, 1 - \varphi_0^2/a^2\right] & \text{for } \varphi_0^2 \lesssim a^2 \\ \dfrac{\omega_0 \pi}{2\ell n(4a/\varphi_0)} & \text{for } \varphi_0^2 \ll a^2. \end{cases} \tag{45}$$

The limiting forms of the trajectories are also easily obtained for small m and for m near unity.

The maxima and minima are stable equilibrium points of the flow, whereas the other roots of $\dot{x} = 0$, $\dot{y} = 0$ at $qx = n\pi$ and $ky = (2m + 1)(\pi/2)$ are unstable equilibrium points in the flow. As shown in Fig. 4, the flows in the neighborhood of an unstable point lie on opposite sides of the separatrix given by $qx = n\pi$ or $ky = (2m + 1)(\pi/2)$. The separatrix is defined by $\varphi(x,y) = 0$, which also defines the only "confined orbits" of the Hamiltonian system. The period of the flow becomes long for contours near the separatrix.

Let us calculate the trajectory of the flow near the separatrix at $ky = \pi/2$ going from $qx = 0$ to π. For $ky = \pi/2$ the equations of motion (41) and (42) become

$$\dot{x} = -\frac{\partial \varphi}{\partial y} = ka \sin(qx)$$

$$\dot{y} = 0 \ ,$$

which integrates as

$$\int_0^{qx(t)} \frac{d(qx')}{\sin(qx')} = \omega_0 \int_{-\infty}^{t} dt' \ .$$

Performing the integral, we obtain the trajectory

$$qx(t) = 2 \tan^{-1}\left[\exp(\omega_0 t)\right]$$

$$= \begin{cases} 0 & \text{at } \omega_0 t = -\infty \\ \pi & \text{at } \omega_0 t = +\infty \end{cases} \qquad (46)$$

The trajectory has an infinite period and its Fourier transform contains all frequencies with its maximum amplitude at zero frequency.

V. PERTURBATIONS AND THE ONSET OF STOCHASTICITY

In Section IV we show that the guiding centers are convected at the frequency $\omega(\varphi_0) = kq(cTe/eB)\hat{\omega}(\varphi_0/a)$ in the plasma by the drift mode $\varphi(x,y)$ whose fundamental component is $\varphi = a \sin(qx) \cos(ky - \omega_k t)$. That part of the flow that is near the separatrix $|\varphi_0| \ll a$ has a long period for circulation. As shown by Chirikov[6] in his Section 4 on motion in the vicinity of the separatrix, the trajectories near the separatrix become stochastic in the presence of a small resonant perturbation. Qualitatively, we expect the perturbation analysis of the pendulum separatrix given in Section 4.4 of Chirikov to apply to the present drift wave problem.

In this section we consider the perturbation calculation of the convection in the primary drift wave due to the presence of a small amplitude secondary wave. In the reference frame moving with the primary wave analyzed in Section IV we consider the perturbation

$$\varphi_1(x,y,t) = a_1 \sin(q_1 x) \cos(k_1 y - \omega'' t) \quad (47)$$

where $\omega'' = \omega_{k_1} - ku = \omega_{k_1} - \omega_k$ with ω_k being the frequency in the laboratory frame. The equations for the perturbations $\delta x(t)$ and $\delta y(t)$ are

$$\delta x(t) = k_1 a_1 \int_{-\infty}^{t} \sin\left[q_1 x_0(t')\right] \sin\left[k_1 y_0(t') - \omega'' t'\right] dt'$$

$$\delta y(t) = q_1 a_1 \int_{-\infty}^{t} \cos\left[q_1 x_0(t')\right] \cos\left[k_1 y_0(t') - \omega'' t'\right] dt' \quad . \tag{48}$$

The secondary wave can arise from the mode-coupling processes.

There are resonant contributions to the perturbations at times $t = t_s$ where the integrals have points of stationary phase given by

$$\pm q_1 \frac{dx_0}{dt}(t_s) \pm k_1 \frac{dy_0}{dt}(t_s) = \omega'' \quad . \tag{49}$$

Condition (49) is an example of the general resonance condition for perturbations acting on a nonlinear oscillator as discussed by Chirikov. Generalizing the condition by treating the two waves with comparable amplitudes leads to the resonance overlap condition for fully stochastic trajectories.

For trajectories sufficiently near the maxima or minima of $\varphi(x,y)$ that the sinusoidal orbit approximation becomes relevant we may estimate the resonance condition to obtain

$$\omega^{n\ell} = am^{\frac{1}{2}} \frac{cT_e}{eB} A > |\omega''| \tag{50}$$

where

$$A = |\underset{\sim}{k}_1 \times \underset{\sim}{k}_2 \cdot \hat{z}| = |q_1 k - k_1 q| \quad .$$

The resonance condition (50) appears easiest to satisfy near the separatrix where $m \sim 1$.

For trajectories near the separatrix we may proceed more directly by following the pendulum calculation in Section 4.4 of Chirikov. The orbit near the separatrix $x_0(t'), y_0(t')$ in the perturbation integral is replaced by the orbit on the separatrix. Considering that part of the orbit that has $ky_0 \cong \pi/2$ and $x_0(t)$ given by equation (46), we obtain for the resonant part of the perturbation

$$\delta x \cong k_1 a_1 \sum \sin(k_1\pi/2k)\, \mathrm{Re} \int_{-\infty}^{+\infty} e^{iq_1 x_0(t') - i\omega'' t'} dt'$$

$$\delta y \cong q_1 a_1 \sum \cos(k_1\pi/2k)\, \mathrm{Im} \int_{-\infty}^{+\infty} e^{iq_1 x_0(t') - i\omega'' t'} dt' .$$

Along the $x_0(t)$ motion the condition for the stationary phase becomes

$$q_1 k \left(\frac{cT_e}{eB}\right) \frac{a}{\cosh(\omega_0 t_s)} = |\omega''| .$$

Repeating the calculation for the motion along $qx_0 = n\pi$ and $y_0(t)$ on the separatrix the resonance condition is

$$k_1 q \left(\frac{cT_e}{eB}\right) \frac{a}{\cosh(\omega_0 t_s)} = |\omega''| .$$

From these results we see that when $\omega^{n\ell} > |\omega''|$ there are stationary points $\pm t_s$ in the perturbation integrals and

thus a resonant interaction occurs. The resonance occurs for a period of time τ_r of order

$$\tau_r \sim \frac{1}{\omega_0 \sqrt{a}} \sim \frac{\sqrt{a}}{\omega^{n\ell}}$$

short compared to $1/\omega^{n\ell}$ for a small a.

In the approximation that the change in position of the guiding center is negligible between resonances, it is possible to write a two-dimensional map for the successive interactions. This map is the analog for this problem of the whisker map for the pendulum problem, which shows that the stochasticity along the separatrix occurs at arbitrarily small perturbation. Without pursuing this calculation in detail it appears evident, and can be observed in examples by numerical integrations, that the flows in the neighborhood of the separatrix become stochastic for very small amplitude perturbations when the resonance condition $\omega^{n\ell} \sim |\omega''|$ is satisfied.

In Fig. 5 we show the effect by adding to the single mode equation the small perturbation $a_1 \sin(q_1 x) \cos(k_1 y - \omega'' t)$. Repeating the integration given in Fig. 4 with $a_1/a \sim 0.03$ and $\omega^{\ell} \sim \frac{1}{2}|\omega''|$ leads to the stochastization of the orbits along the separatrix. In Fig. 5 the $x(t)$, $y(t)$ are plotted every $t_n = 2\pi n/\omega''$. The points along the separatrix are observed to jump from cell to cell in an irregular manner.

In studies of the transition to turbulence in fluids the stochastization of the flow between convective cells appears to have been observed in a recent experiment. In the experiments of Bouabdallah and Cognet[7] on Couette flow, measurements of the autocorrelation function of the fluid oscillations are reported as a function of axial distance across the Taylor vortex cells. The measurements show that the incoherence in the oscillation develops preferentially in the flow between the vortex cells.

The effect is shown in Fig. 6 of Bouabdallah and Cognet[7] where the autocorrelation function of the oscillation is shown for three axial positions corresponding to the two boundaries and the middle of the vortex cell. For the Taylor number (T = 263) below the onset of turbulence the correlation is near unity for all three axial positions, whereas for the intermediate Taylor number (T = 637) the flow is well correlated in the center of the cell and incoherent at the ends of the cell. For a still larger Taylor number (T = 710) the correlation function at all three axial positions decays rapidly with time.

This aspect of the experiments is readily interpreted by the theory for the onset of stochasticity along the separatrix for the Hamiltonian equations (41) and (42) describing the two-dimensional flow. Noting that the equations of motion (41) and (42) are the characteristics for solution of the partial differential equation for (1)

the pressure fluctuation in the toroidal drift-mode problem and (2) the vorticity in the Couette flow problem, it follows that the pressure or the vorticity fluctuations, respectively, become stochastic first in the spatial regions separating the convective cells. Nonlinear fluid simulations of the temperature gradient-driven drift mode also show this behavior as can be seen from the evolution of the flow shown in Fig. 5 of Horton, Estes and Biskamp[1] and in Brock and Horton.[9]

There is also experimental evidence that a resonant perturbation may be producing stochasticity in the circular Couette flow experiments at the University of Texas. From visualization measurements, Gorman[8] has observed the onset of fine-scale structure in the flow. The fine structure occurs approximately with the onset of the second characteristic frequency. Near the onset, the structure is prominent around the boundaries of the cells which we call the separatrix of the flow pattern. Although less well correlated with this onset, there is a definite strengthening of the mixing from cell to cell of the polymeric flakes in this regime of the experiment. Recent laser Doppler shift measurements by Reith and Swinney[10] report a strong correlation of the axial variation of the noise with the location of outward flow between cell boundaries.

VI. CONCLUSION

The nonlinear limit of the toroidal drift instability is investigated in the regime of a single small amplitude mode. Based on the small amplitude $a(t)$ expansion carried out to third, it is shown that within this truncated description the amplitude obeys a simple set of ordinary differential equations. In the absence of dissipation the analytic solution is found as a reversible pulse $a(t)$ with the characteristic limiting amplitude $a_L(\epsilon_n, \eta, q)$ where ϵ_n is the inverse aspect ratio, η the temperature gradient parameter and q is the radial wavenumber of the primary mode. The relationship between the nonlinear pulse and the quasilinear approximation in which $a(t)$ approaches a_L as a stable limit cycle is noted in Section III.C .

With the finite amplitude solution, the convective thermal flux is computed and its characteristic value, given in equation (35), is compared with the value obtained from turbulence theory in Horton, Choi and Tang[2]. In Figs. 2 and 3 we summarize the comparison of the single mode amplitude and thermal flux extrapolated to large temperature gradients with the formulas from turbulence theory. It is shown that with the interpretation of the radial wavenumber as an average value in the turbulent spectrum, the two results agree in their parametric dependence. The extrapolated value for the maximum of the single mode a_L is a factor $2\sqrt{2}$ greater than the

root-mean-square amplitude from turbulence theory. The corresponding factor for the comparison of the thermal flux is 8.

The motion of the guiding centers of the ions and electrons in the low phase velocity toroidal drift mode is given by the one-dimensional nonlinear oscillator equations (41) and (42). The period for convection of the flow around the circumference of a cell in the single mode is given by equation (45) in terms of the elliptic integral. The logarithmic singularity of the period for the flow near the separatrix makes the flow susceptible to small perturbations. Using the trajectory for the guiding center motion along the separatrix, we obtain the condition for large deviations from resonant perturbations. Generalizing the work of Chirikov on the stability of the motion near the separatrix, we find that the condition for the onset of significant stochasticity along the separatrix is given by equation (50).

In Fig. 5 we show the effect of adding a three percent perturbation on the trajectories describing the flow. When the resonance condition is approached, $\omega^{n\ell}(\underset{\sim}{k},\underset{\sim}{k}_1) \leq |\omega_{\underset{\sim}{k}} - \omega_{\underset{\sim}{k}_1}|$, the boundaries of the cells become strongly stochastic with guiding centers moving across the cells in both the radial and azimuthal directions. Since the trajectories are the characteristics of the convective derivative in the dynamical equation for the pressure, the pressure fluctuations

also become stochastic when the resonance condition is satisfied. Here we do not attempt to identify the origin of the perturbation that produces the stochastic motion. We simply note that, in general, the perturbation may arise from the nonlinear dynamic itself.

Finally, we note the important qualitative difference between the onset of stochasticity in the present drift wave problem and that of the stochastic pendulum. In the pendulum, or ordinary plasma wave problem, the Kolmogorof-Arnold-Moser surfaces, at values of the Chirikov overlap parameter less than unity, divide the phase space so as to prevent motion in velocity across the resonances. The resonant surfaces along which the stochasticity starts in the drift wave problem, in contrast, form a two-dimensional rectangular web across the magnetic field as shown in Fig. 5. Now, even at small values of the overlap condition $\omega^{n\ell}/|\omega''|$, given in equation (50), some particles move randomly over many nonlinear resonances in the entire phase space.

Acknowledgments

The author gratefully acknowledges useful discussions with Professor M. N. Rosenbluth and Professor G. Schmidt during the course of this work. The numerical calculations were performed by Mr. Lee Leonard.

This work was supported by the United States Department of Energy, Grant #DE-FG05-80ET 53088.

APPENDIX

In this appendix we generalize the single-mode amplitude equation of Section II to include nonlinear phase oscillations between the pressure and the potential fluctuations. The phase oscillations limit the exponential growth and decay of the amplitude given in equation (29).

Returning to equations (1) and (2) we generalize the form of the solution taken in equations (8) and (9) to

$$\varphi(\underset{\sim}{x},t) = \Phi(x)\left\{\varphi(t)\,\exp[ik(y - ut)] + \varphi^*(t)\,\exp[-ik(y - ut)]\right\} \tag{A.1}$$

$$\delta p(\underset{\sim}{x},t) = \Phi(x)\left\{\delta p(t)\,\exp[ik(y - ut)] + \delta p^*(t)\,\exp[-ik(y - ut)]\right\} \tag{A.2}$$

where again we take $\Phi(x) = \sin(qx)$ with q fixed from the geometry. Equation (2) determines the amplitude and phase of the pressure fluctuation $\delta p(t)$ relative to the potential fluctuation through

$$\delta p(t) = -\left(\frac{u - u_k}{2\varepsilon_n}\right)\varphi - \frac{i}{2\varepsilon_n k}\frac{d\varphi}{dt} \tag{A.3}$$

from which it follows that

$$\varphi\delta p^* - \varphi^*\delta p = \frac{i}{2\varepsilon_n k}\frac{d}{dt}|\varphi|^2 \quad . \tag{A.4}$$

Calculating the $\underset{\sim}{v}_E\cdot\nabla\delta p$ convection as in equation (19), we obtain

$$\frac{d}{dt}\,\delta p^{(2)} = -iqk\,\sin(2qx)(\varphi\delta p^* - p\varphi^*) \quad , \tag{A.5}$$

where again the $\exp[2ik(y - ut)]$ variation cancels.

Using equation (A.4) we may integrate equation (A.5) to obtain

$$\delta p^{(2)} = \frac{q}{2\varepsilon_n} \sin(2qx) \left[|\varphi(t)|^2 - |\varphi(0)|^2 \right] . \qquad (A.6)$$

Repeating the third-order analysis in Section II.B now gives the nonlinear oscillator equation

$$\frac{d^2\varphi}{dt^2} - 2i\Omega_k \frac{d\varphi}{dt} - k^2 \left[u(u - u_k) + \gamma_0^2 - q^2 |\varphi(t)|^2 \right] \varphi = 0 \qquad (A.7)$$

where $\Omega_k = k(u - \frac{1}{2}u_k)$ is the frequency shift from the linear frequency $\frac{1}{2}ku_k$ in the unstable domain $2\gamma_0 \gtrsim |u_k|$. At small amplitudes the oscillator (A.7) gives the wave dispersion relation $\omega(\omega - ku_k) + k^2\gamma_0^2 = 0$ with $\omega = ku$ and the constant amplitude $\ddot{\varphi} = \dot{\varphi} = 0$. In equation (A.7) we restrict consideration to initial data for which $|\varphi(0)| \ll \gamma_0/q$.

In the unstable domain we introduce the discriminant of the linear dispersion relation through $\gamma_k^2 = k^2(\gamma_0^2 - \frac{1}{4}u_k^2)$ and transform away the dependence on Ω_k by introducing $\varphi(t) = \psi(t) \exp(i\Omega_k t)$ to obtain

$$\frac{d^2\psi}{dt^2} - \left[\gamma_k^2 - k^2 q^2 |\psi|^2 \right] \psi(t) = 0 . \qquad (A.8)$$

In terms of amplitude and phase variables $\psi(t) = a(t) \exp[i\alpha(t)]$ we obtain from equation (A.8) the phase integral

$$a^2(t) \frac{d\alpha}{dt} = \text{const.} = a_0^2 \alpha_0 \qquad (A.9)$$

and from the amplitude equation

$$\frac{d^2a}{dt^2} = -\frac{\partial V}{\partial a}$$

with the energy integral

$$\frac{1}{2}\left(\frac{da}{dt}\right)^2 + V(a) = E \qquad \text{(A.10)}$$

where

$$V(a) = \frac{1}{2}\frac{a_0^4\dot{\alpha}_0^2}{a^2} - \frac{1}{2}\gamma_k^2 a^2 + \frac{1}{4}k^2q^2a^4 \quad . \qquad \text{(A.11)}$$

It is convenient to follow equations (28) through (30) by introducing the scaled squared amplitude $x(\tau) = a^2(t)/a_L^2$ where $a_L = \sqrt{2}\ (\gamma_k/kq)$ and the scaled time $\tau = 2\gamma_k t$ to obtain

$$\frac{dx}{d\tau} = \pm\left[\varepsilon x - \nu_0^2 + x^2(1 - x)\right]^{1/2} \qquad \text{(A.12)}$$

where ε and ν_0 are the rescaled constants of integration in equations (A.9) and (A.10) given by $\varepsilon = k^2q^2E/2\gamma_k^4$ and $\nu_0^2 = a_0^4\dot{\alpha}_0^2k^4/4\gamma_k^6$.

The general $x(\tau)$ depends on the constants of integration ε, ν_0 through the roots of cubic $x^2(x - 1) - \varepsilon x + \nu_0^2 = 0$. The motion of most interest appears when ε, $\nu_0 << 1$ which describes the first departure from the exponential pulse $a(t)$ obtained in the text.

For small ν_0 the motion occurs between the maximum root $x_1 \simeq 1$ and the positive root of the approximate pair of roots at $x_{2,3} = \pm(\nu_0^2 + \frac{1}{4}\varepsilon^2)^{\frac{1}{2}} - \frac{1}{2}\varepsilon$. The index of the

elliptic function is $m = (x_1 - x_2)/(x_1 - x_3)$ and the phase is $\theta = \frac{1}{2}(x_1 - x_3)^{\frac{1}{2}}\tau$.

The integral of equation (12) is

$$x(\theta) = \frac{x_2 - x_3 msn^2\theta}{1 - msn^2\theta} = \frac{x_2 - x_3 msn^2\theta}{dn^2\theta} \qquad (A.13)$$

where at $\theta = \tau = 0$, $x = x_2$ and at $\theta = \frac{1}{2}(x_1 - x_3)^{\frac{1}{2}}\tau = K(m)$, $x = x_1 \simeq 1.0$. For small ε and ν_0 we have $m = (1 - \nu_0)/(1 + \nu_0) \lesssim 1$, and we obtain the exponential limit of the elliptic functions. Using these limits and that $x_2 \simeq \nu_0 \simeq a^2(0)/a_L^2$, we recover the exponential pulse

$$a(t) = a(0)\left[\frac{a^2(0) + a_L^2 \cosh(\gamma_k t)}{a_L^2 + a^2(0) \cosh(\gamma_k t)}\right]^{1/2} \qquad (A.14)$$

with the finite period. Taking into account the translation in the reference time at which $\max a(t) = a_L$ this result (A.14) is equivalent to that given in the text.

References

1. W. Horton, R. D. Estes and D. Biskamp, Plasma Phys. 22, 663 (1980).

2. W. Horton, D. I. Choi and W. M. Tang, Phys. Fluids 24, 1077 (1981).

3. F. L. Hinton, et al. in Proc. 8th Int. Conf. on Plasma Physics and Controlled Nuclear Fusion (IAEA, Vienna, 1981). Vol. I, p. 365.

4. H. B. Keller, "Numerical Solution of Bifurcation and Nonlinear Eigenvalue Problems", in Applications of Bifurcation Theory, (P. Rabinowitz, ed.), Academic Press, New York, (1977), pp. 359-384.

5. B. Coppi and F. Pegoraro, Nucl. Fusion 17, 5 (1977).

6. B. V. Chirikov, Physics Reports 52, 263 (1979).

7. A. Bouabdallah and G. Cognet, "Laminar-Turbulent Transition in Taylor Couette Flow", in Proc. of I.V.T.A.M. Symposium on Laminar-Turbulent Transition, (Stuttgart, 1979).

8. M. A. Gorman (private communication).

9. D. Brock and W. Horton, "Evolution of Toroidal Drift Wave Fluctuations", Institute for Fusion Studies, University of Texas at Austin, IFSR#32, July 1981, to be published in Plasma Physics.

10. L. A. Reith and H. L. Swinney, "Axial Measurements of the Noise in Couette Flow", to be published.

Figure Captions

Fig. 1 The unstable range of azimuthal wavenumbers as a function of increasing temperature gradient is shown in (a) with one mode unstable and (b) two modes unstable. Fig. 1c shows a typical sequence for bifurcations in the amplitudes of the nonlinear oscillations as a function of increasing temperature gradient.

Fig. 2 The parametric dependence of the single mode amplitude $a_L(\eta,\varepsilon_n,q)$ compared with the root-mean-square amplitude from renormalized turbulence theory.

Fig. 3 Thermal conductivity as a function of the temperature gradient showing three regimes: (1) conduction for $\eta < \eta_c$, (2) convection with a collisional phase shift $\eta_c < \eta < \eta_c'$, and (3) convection with a collisionless phase shift $\eta > \eta_c'$.

Fig. 4 Convective motion of the guiding centers in the single drift mode with amplitude a_L.

Fig. 5 Onset of stochasticity in the flow along the separatrix due to the addition of a small perturbation (3%) with comparable wavenumbers.

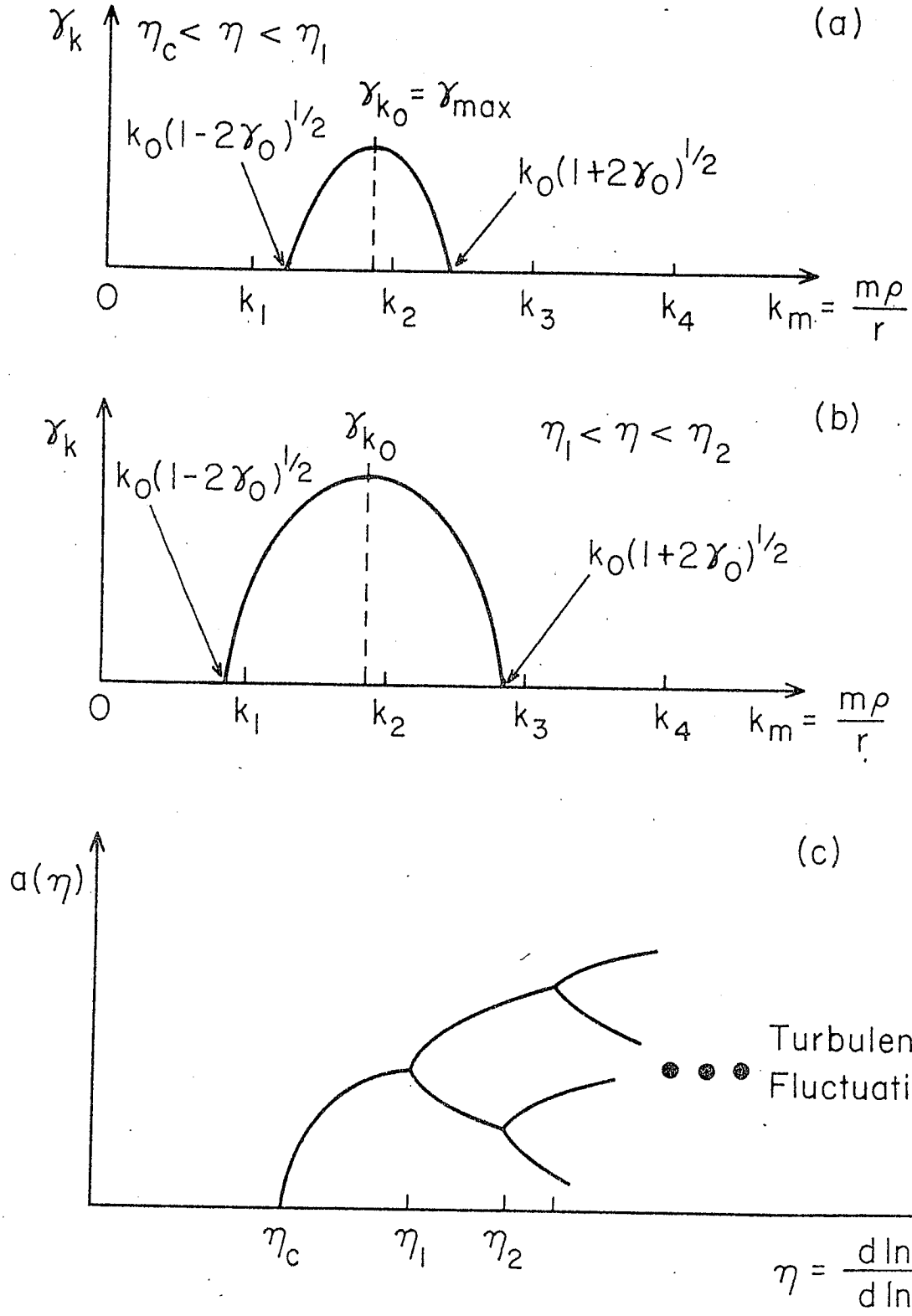
γ_k
$\eta_c < \eta < \eta_1$
(a)
$\gamma_{k_0} = \gamma_{max}$
$k_0(1-2\gamma_0)^{1/2}$
$k_0(1+2\gamma_0)^{1/2}$
O
k_1
k_2
k_3
k_4
$k_m = \frac{m\rho}{r}$
γ_k
γ_{k_0}
$\eta_1 < \eta < \eta_2$
(b)
$k_0(1-2\gamma_0)^{1/2}$
$k_0(1+2\gamma_0)^{1/2}$
O
k_1
k_2
k_3
k_4
$k_m = \frac{m\rho}{r}$
$a(\eta)$
(c)
Turbulent
Fluctuations
η_c
η_1
η_2
$\eta = \frac{d\ln T}{d\ln n}$

FIG. 1

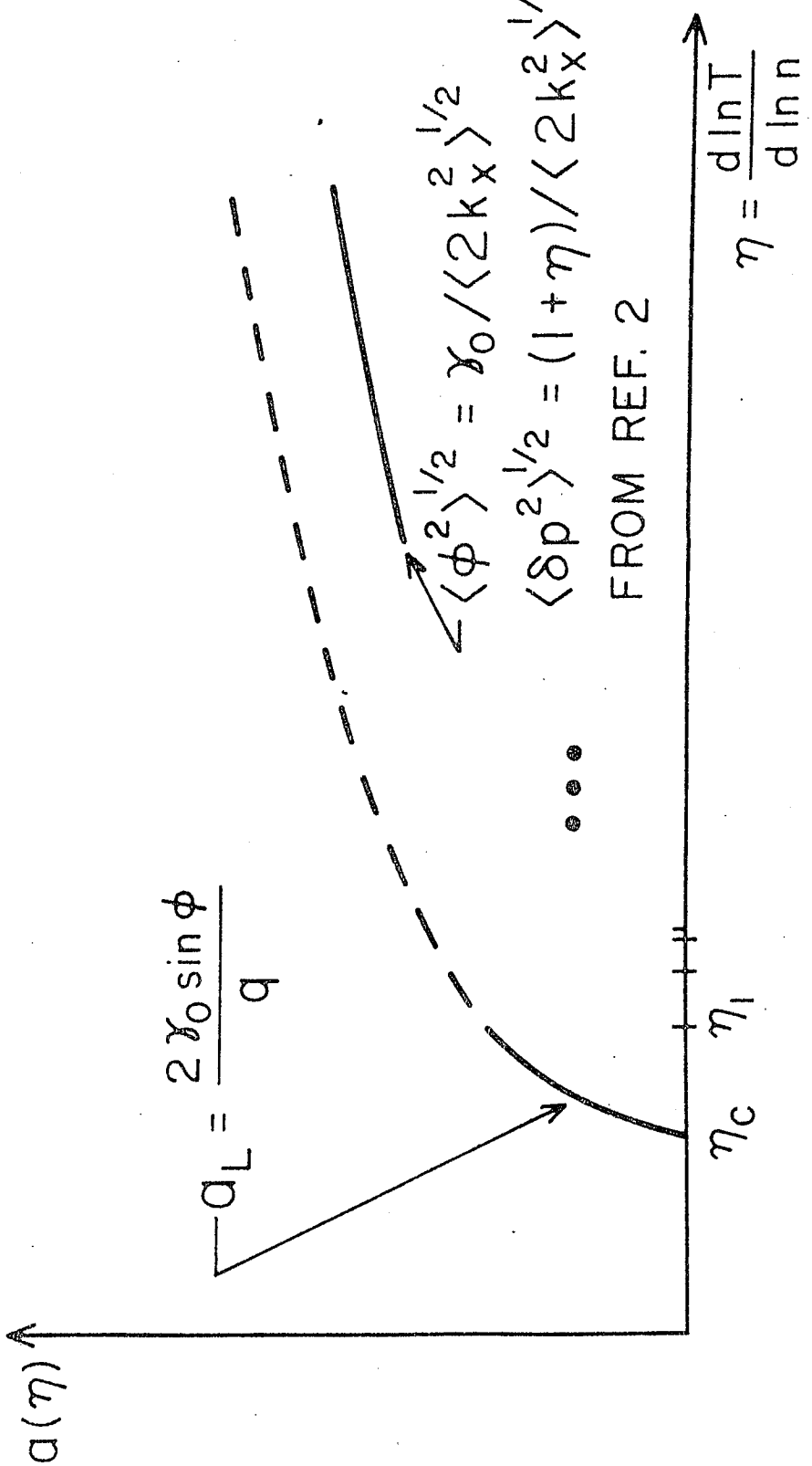
a(η)
$a_L = \frac{2\gamma_0 \sin\phi}{q}$
$\langle\phi^2\rangle^{1/2} = \gamma_0/\langle 2k_x^2\rangle^{1/2}$
$\langle\delta p^2\rangle^{1/2} = (1+\eta)/\langle 2k_x^2\rangle^{1/2}$
FROM REF. 2
$\eta = \frac{d\ln T}{d\ln n}$
η_c
η_1

FIG. 2

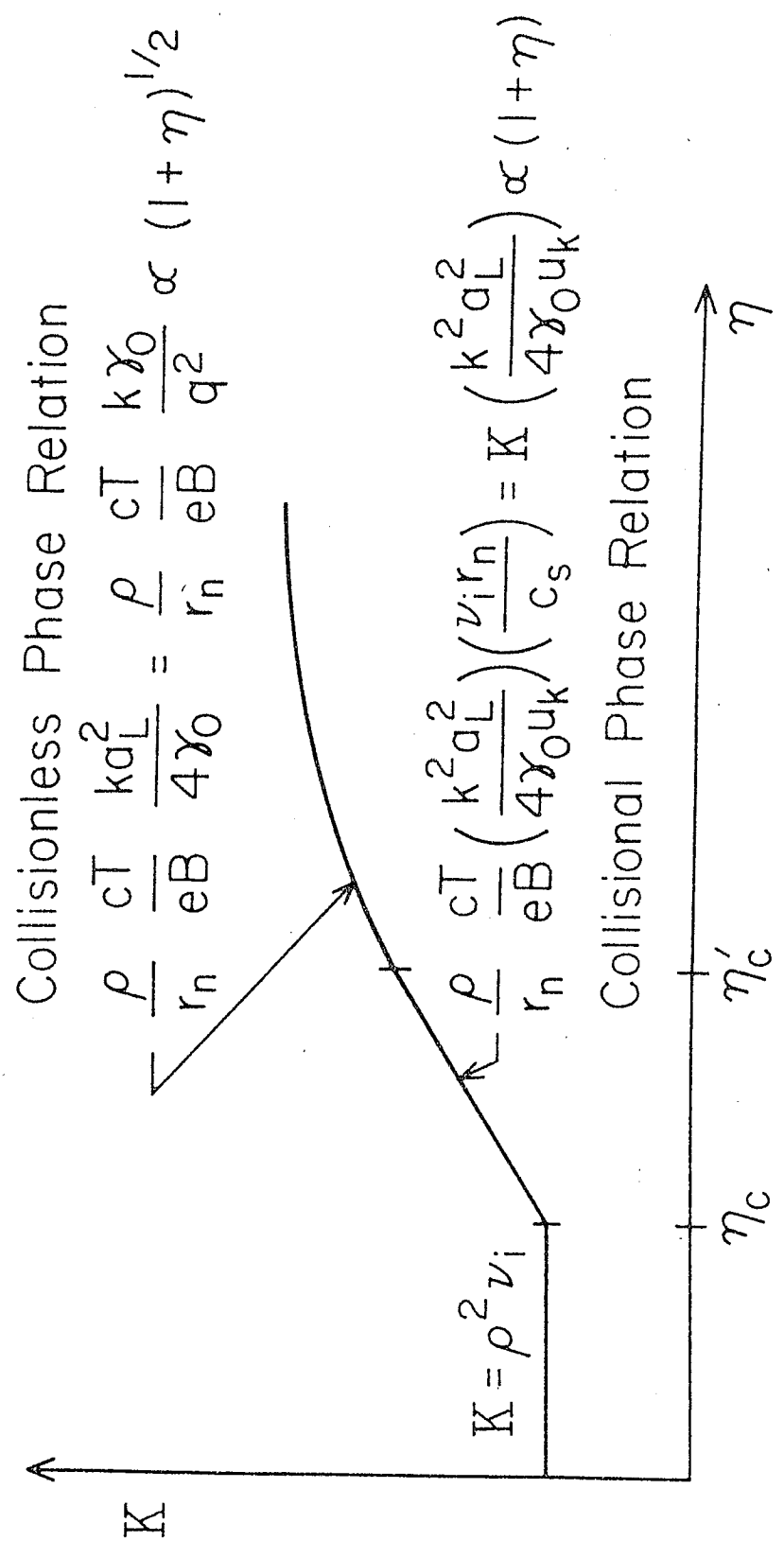
Collisionless Phase Relation
$\frac{\rho}{r_n}\frac{cT}{eB}\frac{ka_L^2}{4\gamma_0} = \frac{\rho}{r_n}\frac{cT}{eB}\frac{k\gamma_0}{q^2} \propto (1+\eta)^{1/2}$
$\frac{\rho}{r_n}\frac{cT}{eB}\left(\frac{k^2a_L^2}{4\gamma_0 u_k}\right)\left(\frac{\nu_i r_n}{c_s}\right) = K\left(\frac{k^2a_L^2}{4\gamma_0 u_k}\right) \propto (1+\eta)$
Collisional Phase Relation
$K = \rho^2\nu_i$
K
η
η_c
η_c'

FIG. 3

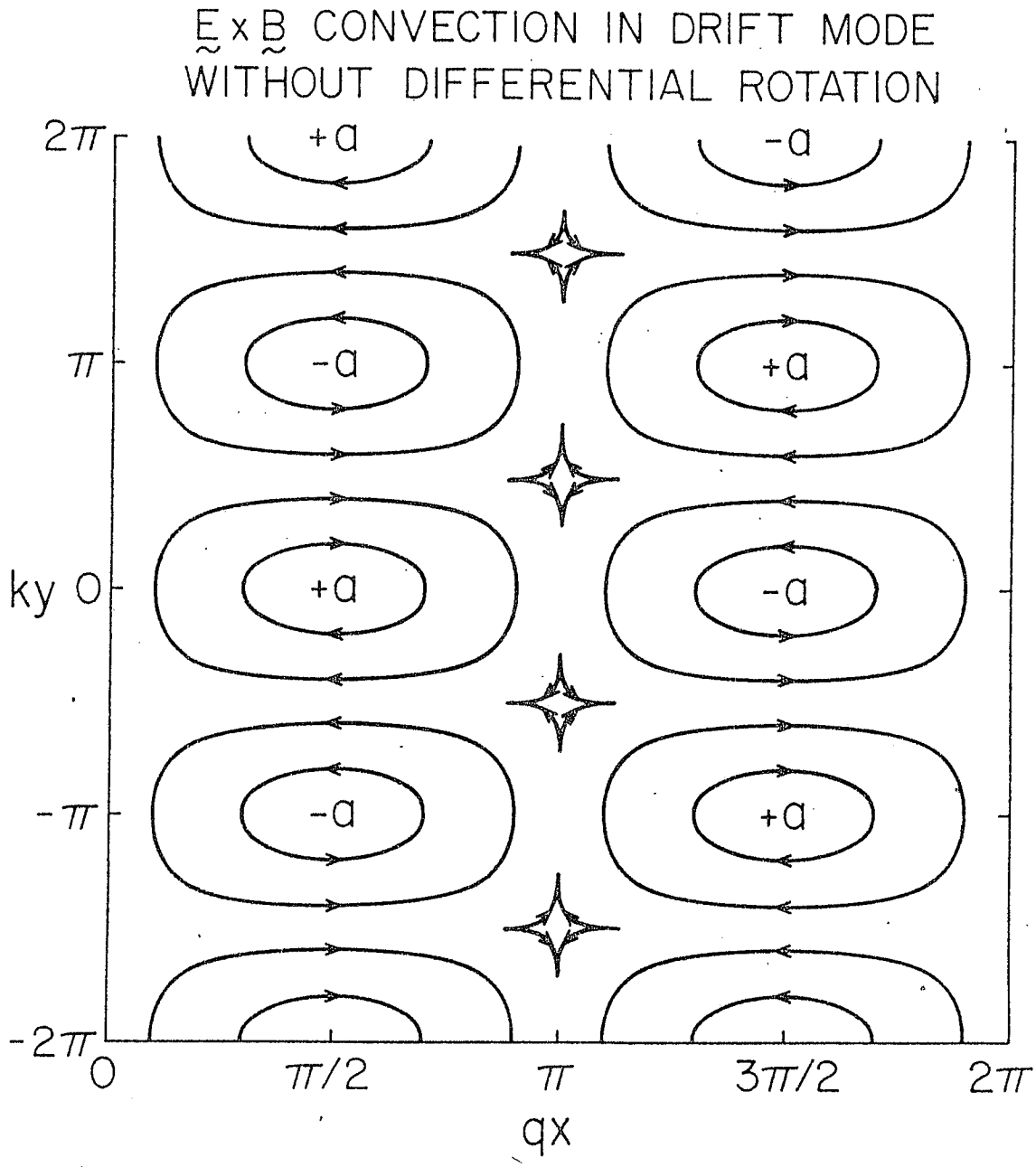
E x B CONVECTION IN DRIFT MODE
WITHOUT DIFFERENTIAL ROTATION
2π
π
ky 0
-π
-2π
+a
-a
-a
+a
+a
-a
-a
+a
0
π/2
π
3π/2
2π
qx

FIG. 4

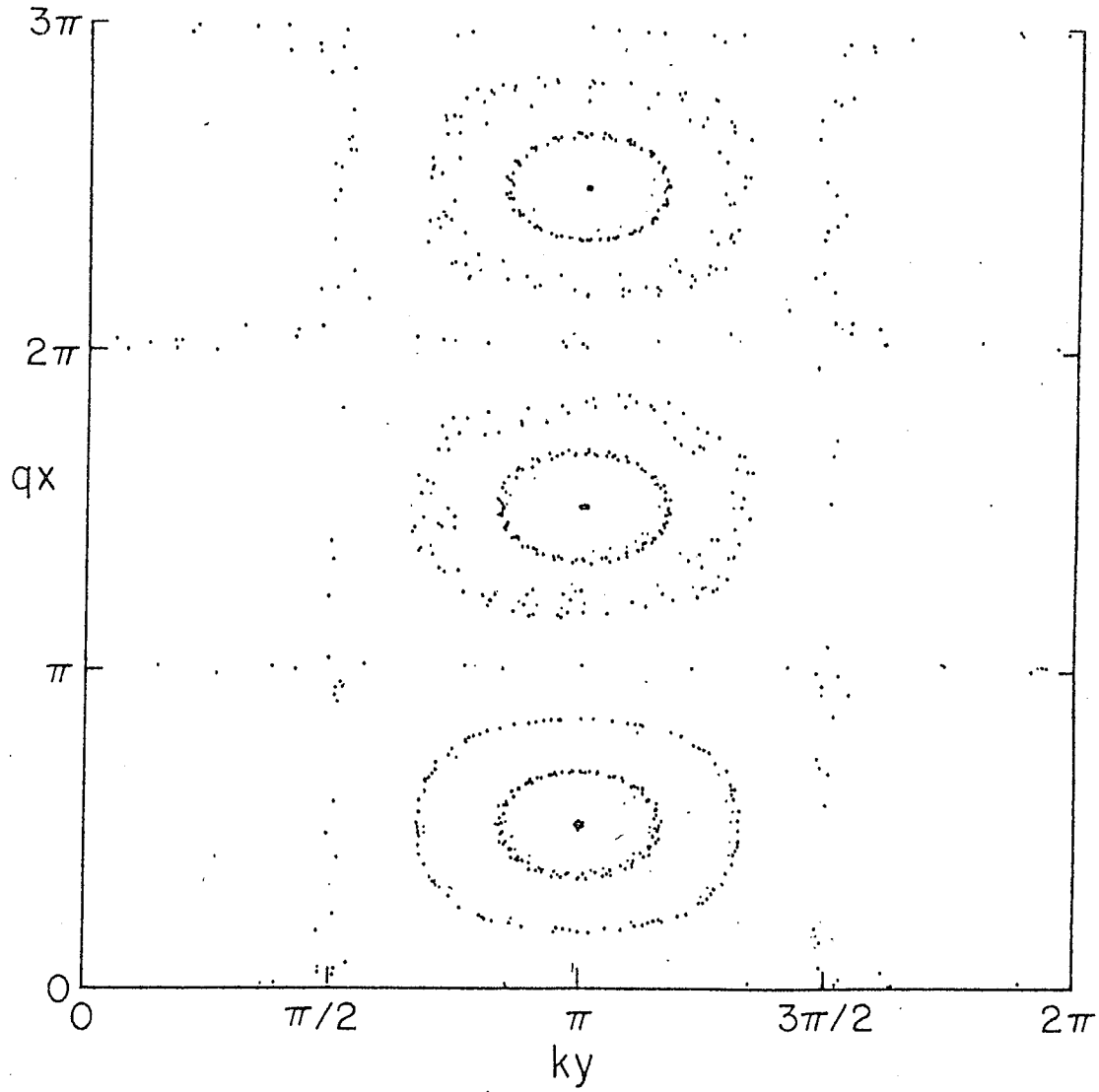

FIG. 5